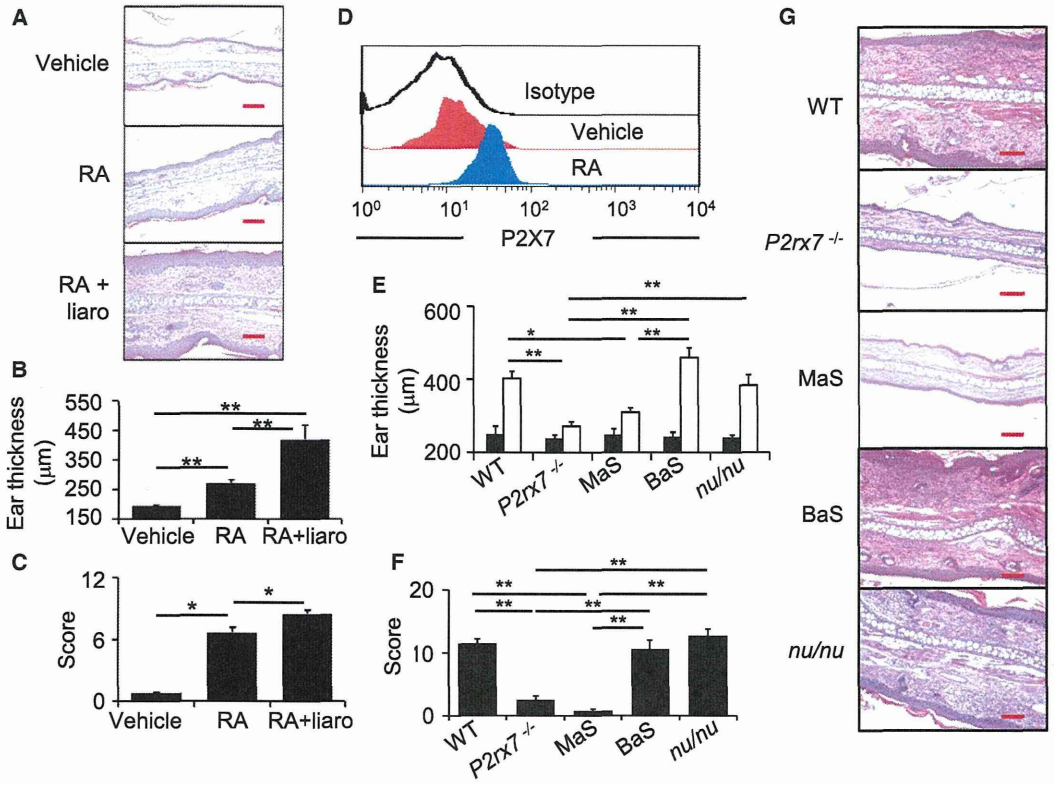

Figure 5. Aberrant P2X7 Expression in Mast Cells Induces Retinoid Dermatitis

(A) Hematoxylin and eosin (H&E) staining of skin from mice treated with vehicle or RA with or without liarozole (liaro) for 2 weeks. Data are representative of at least three independent experiments. Scale bars represent 100 μm.

(B) Thickness of ear was measured. Data are means ± SEM. $^{**}p < 0.01$ (n = 4).

(C) Severity of inflammation was scored. Data are means ± SEM. $^{*}p < 0.05$ (n = 4).

(D) Expression of P2X7 on skin MCs in RA- or vehicle-treated mice was examined by flow cytometry analysis.

(E) Mice (WT; diphtheria toxin-treated MaS-TRECK, MaS; diphtheria toxin-treated BaS-TECK, BaS; and nude; *nu/nu*) were treated with RA for 8 weeks and ear thickness was measured (n = 6 to 24).

(F) Severity of inflammation was scored (n = 3 to 4) (means ± SEM. $^{*}p < 0.05$, $^{**}p < 0.01$, one-way ANOVA and Tukey's method).

(G) Representative H&E staining of ear are shown. Scale bars represent 100 μm.

suprabasal layers, eventually leading to retinoid dermatitis (Fisher and Voorhees, 1996; García-Serrano et al., 2011). Additionally, skin irritation occurs with retinoid treatment (Varani et al., 2003). High-dose oral administration of RA to pregnant mice causes skin inflammation in the fetus (Okano et al., 2012). These findings led to a hypothesis that P2X7 expression on skin MCs induced by high concentration of RA might be of relevance to skin irritation or retinoid dermatitis.

To test this hypothesis, mice were orally inoculated with 0.4% RA twice a week for several weeks. These RA-treated mice showed skin irritation and hypertrophy when compared with vehicle-treated mice (Figures 5A–5C; Figure S4A). Histological analysis showed that RA treatment caused dermatitis associated with the accumulation of inflammatory cells and MCs (Figures 5A; Figure S4B–S4E). Importantly, P2X7 expression in skin MCs in RA-treated mice was augmented compared with that in vehicle-treated mice (Figure 5D). Moreover, inhibition of Cyp26b1-dependent RA metabolism by the treatment with liarozole exacerbated the skin inflammation compared with RA treatment alone (Figures 5A–5C; Figure S4B). These results indicated that Cyp26b1 counteract the onset of RA-induced dermatitis. Furthermore, RA-induced dermatitis was ameliorated in *P2rx7*$^{-/-}$- and MC-deficient mice, but not in basophil-deficient mice (Figures 5E–5G).

We confirmed a previous report (Hall et al., 2011) that RA induces the differentiation of both T helper 17 (Th17) and regulatory T cells (Figure S4F). RA treatment also slightly induced P2X7 expression on skin T cells (Figure S4G). Therefore, to evaluate the possible involvement of T cells in the induction of RA-induced dermatitis, we analyzed T cell-deficient nude (*nu/nu*) mice (Figures 5E–5G). We observed ear swelling accompanied by inflammation in *nu/nu* mice (Figures 5E–5G), indicating that, even though RA treatment affected the P2X7 expression in both T cells and MCs, MCs play central roles in the induction of retinoid dermatitis.

To examine the expression of P2X7 ligands in retinoid dermatitis, we next measured the production of extracellular ATP—a major ligand of P2X7—in mice with retinoid dermatitis or mice receiving skin scratch as a control (Kawamura et al., 2012). We detected elevated amounts of ATP in the skin of mice with

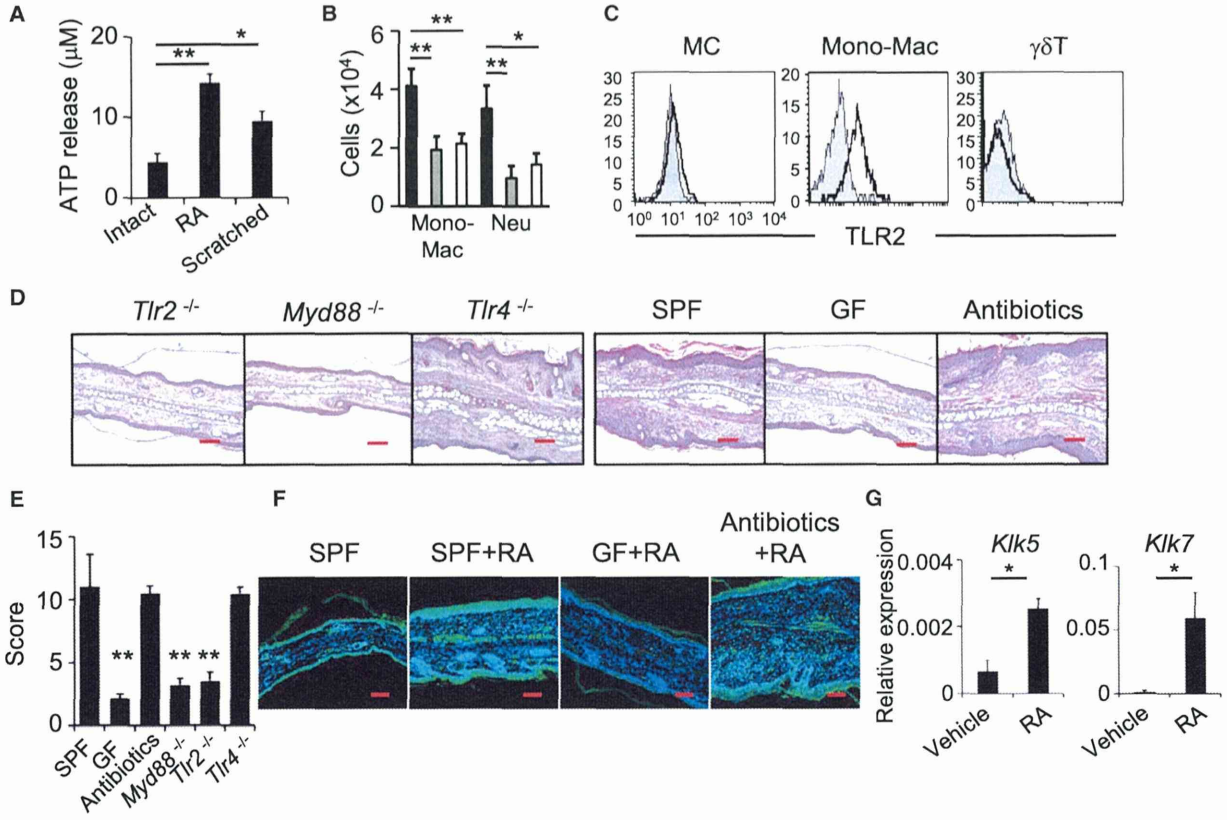

Figure 6. Skin Commensal Bacteria Contribute to P2X7-Medaited Retinoid Dermatitis

(A) ATP concentrations released from skin tissues were measured (means ± SEM. *$p < 0.05$; **$p < 0.01$).

(B) The numbers of monocytes and macrophages (Mono-Mac) and neutrophils (Neu) in the skin after RA-treatment were quantified (black bars, WT; gray bars; *P2x7*$^{-/-}$; white bars, diphtheria toxin-treated MaS-TRECK mice) (means ± SEM. *$p < 0.05$; **$p < 0.01$).

(C) TLR2 expression was examined in MCs, CD11b^{+} Mono-Mac, and γδ T cells. Control staining with isotype control antibody is shown as gray.

(D) *Tlr2*$^{-/-}$, *Myd88*$^{-/-}$, and *Tlr4*$^{-/-}$, specific-pathogen-free (SPF), germ-free (GF), and antibiotic-treated mice were treated with retinoic acid for 8 weeks; representative hematoxylin and eosin staining of ear are shown. Data are representative of at least three independent experiments. Scale bars represent 100 μm.

(E) Severity of inflammation was scored (n = 4 to 6). Data are means ± SEM. **$p < 0.01$; one-way ANOVA and Tukey's method.

(F) Cathelicidin (green) expression was measured by confocal microscopy. Scale bars represent 100 μm.

(G) Kallikrein (KLK) 5 (n = 9) and 7 (n = 4) expression was examined by qRT-PCR. Data are means ± SEM. *$p < 0.05$.

retinoid dermatitis as scratched skin (Figure 6A). In addition, degradation of extracellular ATP by local administration of apyrase suppressed at least partly the severity of retinoid dermatitis (Figures S5A–S5C). The ATP-P2X7 pathway leads to the production of lipid mediators (e.g., leukotriene B4) and chemokines (e.g., MCP1, CCL7, and CXCL2) from MCs to recruit inflammatory cells such as monocytes and neutrophils (Kurashima et al., 2012). We found that CD11b^{+} monocytes and macrophages and Gr-1^{+} neutrophils were increased in the skin of mice treated with RA, but their abundance was lower in RA-treated mice lacking P2X7 or MCs (Figure 6B). These results suggest that increased ATP production in the RA-treated skin caused P2X7- and MC-dependent skin inflammation.

P2X7-Mediated Retinoid Dermatitis Requires Innate Immune Signaling

External stimuli—especially antimicrobial signaling—can provoke or inhibit skin inflammation (Jin et al., 2009). We found that TLR2 was highly expressed by the accumulated cells (e.g., monocytes and macrophages) but relatively low in MCs and γδ T cells (Figure 6C). To determine whether microbial stimulation via TLR2 participated in the induction of retinoid dermatitis, *Tlr2*$^{-/-}$ and *Myd88*$^{-/-}$ mice were inoculated with a high dose of RA. Those mice had only minor incidence of retinoid dermatitis after 8 weeks of RA inoculation, whereas identically treated *Tlr4*$^{-/-}$ mice had typical signs of retinoid dermatitis (Figures 6D and 6E). These results suggest that signaling from TLR2 contributes to the development of retinoid dermatitis. It remains unclear whether TLR2 signaling is mediated by microbial components, because other endogenous ligands, such as hyaluronan fragments, biglycan, and serum amyloid A, also activate TLR2 (Erridge, 2010). Therefore, to determine the requirement for TLR2 ligands derived from skin microbiota, we induced retinoid dermatitis in GF mice. In addition, we used mice receiving antibiotics orally because, unlike GF mice, which were free from both gut and skin microbiota, oral antibiotic administration rarely

influences the skin microbiota but diminishes the gut microbiota (Naik et al., 2012). Whole-mount fluorescent in situ hybridization (FISH) analysis with EUB338 (a probe for most bacterial species) confirmed the presence of skin bacteria in antibiotic-treated mice, but not in GF mice (Figure S5D). When these two groups of mice were subjected to retinoid dermatitis, inflammatory signs were found in the antibiotic-treated mice, but not GF mice (Figures 6D and 6E). These findings suggest that recruitment and activation of $TLR2^+$ monocytes and macrophages by skin microbiota are important for the aggravation of retinoid dermatitis.

Not only ATP but also the cathelicidin-derived peptide LL37 directly activates P2X7 (Elssner et al., 2004). Moreover, bacterial components such as lipoteichoic acid, a ligand of TLR2, induce cathelicidin production (Yamasaki et al., 2007). Indeed, we found that expression of gene encoding *cathelicidin* were low in GF mice subjected to retinoid dermatitis induction, but they were unaltered in antibiotic-treated mice with retinoid dermatitis, compared with SPF mice (Figure 6F). In addition, in vitro analysis revealed that inflammatory monocytes increased the extracellular ATP production and cathelicidin expression via TLR2-dependent manner (Figures S5E and S5F). Kallikrein (KLK) 5 and 7 are required to process cathelicidin to produce LL37 in the skin (Morizane et al., 2010). We found that RA treatment upregulated the expression of both *Klk5* and *Klk7* in the area of retinoid dermatitis (Figure 6G). Furthermore, another in vitro analysis indicated that *Cxcl1* and *Cxcl2* expression was increased in MCs when they were cocultured with monocytes activated via TLR2 (Figure S5G). These observations indicated that cross-communication between skin microbiota- and TLR2-dependent production of P2X7 ligands such as ATP and LL37 from inflammatory monocytes and the activation of MCs via P2X7 is critical for the development of retinoid dermatitis.

DISCUSSION

Skin and mucosa possesses immunologically unique regulatory systems that create balanced homeostatic conditions in the face of the harsh outside environment. It was suggested that tissue environmental factors regulate locally unique MC phenotypes (Xing et al., 2011). As protease expression patterns on MCs (Xing et al., 2011), our previous findings suggested that P2X7 expression on MCs differs between the skin and intestine (Kurashima et al., 2012). Here, we found a function of skin fibroblasts in reducing the P2X7 expression on MCs through the metabolism of RA. This pathway creates unique niches for regulating the homeostatic network of the skin-surface barrier by inhibiting excessive ATP-mediated activation of MCs. We also proposed the possible involvement of LL37 as another ligand of P2X7 in skin inflammation. These observations reveal the unique tissue-dependent immune regulation mediated by structural cells such as stromal cells and fibroblasts to create homeostasis at the skin-surface barrier. Breakdown of this system leads to the development of inflammation such as retinoid dermatitis.

Activation of MCs is tightly regulated by multiple receptors. For instance, elevated expression of IL-33 from epidermal keratinocytes and dermal fibroblasts as a result of sun exposure induces MC activation and hence skin inflammation (Lunderius-Andersson et al., 2012). Simultaneously, various inhibitory receptors, such as leukocyte monoimmunoglobulin-like receptor 3 and paired immunoglobulin-like receptor B, are typically expressed on MCs (Izawa et al., 2012; Masuda et al., 2007). Along with the expression of these inhibitory receptors, regulation of the expression of activation-type receptors such as P2X7 might be important for inhibiting the abnormal activation of MCs under tissue-specific environment, for example at sites where ligands (e.g., ATP and LL37) are constantly or easily produced. Our results showed that TLR2-mediated activation was involved in extracellular ATP release and simultaneous enhancement of LL37 production by monocytes or macrophages. Furthermore, MCs produced ATP via the actions of ATP synthase and adenylate kinase (Kurashima et al., 2012). Thus, extracellular ATP is released from a various sources at millimolar concentration, which are sufficient for P2X7-mediated MC activation at the site of skin inflammation (Takahashi et al., 2013). Therefore, the balanced and optimal expression of activation and inhibitory receptors, as well as ligand production, is required to maintain homeostasis, which was tissue dependent. From this perspective, our findings provide evidence for the presence and mechanism of skin-specific negative regulation of ATP-mediated MC activation via the downregulation of P2X7.

RA has been used clinically to normalize skin homeostasis in patients with acne or psoriasis (Geria and Scheinfeld, 2008). However, topical application of excessive amounts of RA accelerates skin inflammation (Fisher and Voorhees, 1996). Treatment with excessive amounts of 9-*cis* RA causes epidermal proliferation and increased skin thickness in mice (García-Serrano et al., 2011). Furthermore, Cyp26b1 deficiency in keratinocytes and fibroblasts causes skin barrier disruption and inflammation in mice (Okano et al., 2012). Our study indicated the importance of RA-mediated upregulation of P2X7 on MCs in the development of skin inflammation. Liarozole inhibits RA metabolism with targeting not only Cyp26b1 but other P450 enzymes; thus, off-target effects of liarozole could not be negligible (De Coster et al., 1996). Our data indicated the highest expression of Cyp26b1 in skin fibroblasts; these data, plus those from the studies mentioned above, reflect the important aspects and kinetics of the skin fibroblast-Cyp26b1-mediated regulatory and inhibitory system for creating and maintaining a physiologically optimized skin-surface barrier system.

Mcpt expression is reversibly regulated by the tissue environment (Xing et al., 2011). Our data indicate that RA does not regulate Mcpt expression, suggesting that the soluble signals emanating from stromal cells and fibroblasts for MC differentiation and for downregulation of P2X7 expressions differ from each other. Our current findings also revealed that coculture with lung fibroblasts partially reduced P2X7 expression in BMMCs. This effect on P2X7 expression was weaker than that of skin fibroblasts; moreover, P2X7 suppressive capacity was correlated with reduced expression of Cyp26b1 (data not shown). Because concentrations of extracellular ATP were high in respiratory inflammation and lung MCs in vivo expressed high P2X7 (Idzko et al., 2007), reducing P2X7 expression on MCs by enhancing Cyp26b1 expression in fibroblasts in the lung would be a therapeutic strategy for respiratory disorders.

MCs are involved in various skin inflammation, such as psoriasis, atopic dermatitis, and alopecia areata (Cetin et al., 2009; Gilfillan and Beaven, 2011; Otsuka et al., 2011). In this context, high vitamin A concentration in serum is associated with a risk

of atopic dermatitis (Kull et al., 2006). In addition, it was recently reported that dietary vitamin A is involved in aggravating chronic inflammatory status in alopecia both in mice and human (Duncan et al., 2013). In mice with alopecia areata, RA synthesis is increased and simultaneously RA degradation is decreased, thus resulting in excess concentrations of RA at the site of skin inflammation (Duncan et al., 2013). Indeed, P2X7$^+$ MCs are accumulated at the site of alopecia in human (data not shown). These results imply that dysregulation of P2X7 expression on MCs occurs in particular skin inflammation associated with disruption and interruption of RA metabolism. Therefore, it is possible that RA-induced P2X7–MC cascades are also involved in the RA-related skin inflammation.

Skin-resident bacteria play an autonomous role in controlling the local inflammatory milieu by modulating the function of skin-resident T cells (Naik et al., 2012). Functional TLRs are expressed on MCs (Matsushima et al., 2004; Sandig and Bulfone-Paus, 2012). In addition, cathelicidin expression on MCs is induced by the activation of TLR2 by lipoteichoic acid produced by commensal bacteria. Indeed, TLR2 is highly expressed on BMMCs (Wang et al., 2012). Therefore, it is possible that P2X7 and TLR2 dual pathways affect the skin MC-induced production of inflammatory mediators. However, our experiments with three different clones (6C2, mT2.7, and mT2.5) of anti-TLR2 monoclonal antibodies revealed that TLR2 was poorly expressed on the surfaces of skin MCs. Indeed, reconstitution of TLR2-deficient MCs to the MC-deficient mice showed retinoid dermatitis after RA-treatment (data not shown). In contrast, CD11b$^+$ monocytes and macrophages in the skin highly expressed TLR2, indicating that skin-microbiota-mediated signaling stimulates accumulation and activation of inflammatory cells in the skin; this might initiate disruption of skin homeostasis, including the skin fibroblast-Cyp26b1-mediated downregulation system of P2X7-dependent MC activation. In addition, recruitment or activation of the TLR2-expressing inflammatory cells is led by chemokines (e.g., MCP1) or lipid mediators (e.g., leukotrienes) released upon MC activation and the induction of inflammatory responses by ATP release. MCs also directly regulate DC activation in the skin; indeed, maturation and migration of DCs are regulated by TNF-α and ICAM1 on MCs; thus, MC-DC direct interaction could also affect the pathogenesis of skin inflammation (Otsuka et al., 2011). Our in vitro observation revealed that TLR2$^+$ inflammatory cells directly enhanced CXCL1 and CXCL2 expression in MCs, which potentially led to the neutrophil recruitment into the inflammatory site. These results implied the existence of the inflammatory loop among various immune cells including MCs.

These findings collectively reveal that MCs in various tissues help to create tissue-specific local homeostasis operated by individual structural cells (e.g., fibroblasts). Cyp26b1-expressing skin fibroblasts thus play a central role in homeostatic P2X7 downregulation on skin MCs, leading to the suppression of ATP-induced abnormal activation. When the skin homeostatic pathway is sporadically interrupted, such as in hypervitaminosis A, skin bacterial stimulation triggers inflammation via the TLR2-mediated pathway. Our additional understanding of the molecular and cellular bases of the functions and phenotypes of localized MCs and their surrounding structural cells (e.g., fibroblasts and stromal cells) will facilitate the discovery of innovative and beneficial targets for the control of tissue-specific inflammation.

EXPERIMENTAL PROCEDURES

Mice

C57BL/6, Balb/c, GF, and *nu/nu*$^{-/-}$ mice were purchased from Japan CLEA. *Rag1*$^{-/-}$, *Tcrb*$^{-/-}$, *Tcrd*$^{-/-}$, *Ighm*$^{-/-}$, *P2rx7*$^{-/-}$, and *Itgax*-DTR mice were obtained from Jackson Laboratory. *Tlr2*$^{-/-}$, *Tlr4*$^{-/-}$, and *Myd88*$^{-/-}$ mice were obtained from Dr. S. Akira (Osaka University). *Id2*$^{-/-}$ mice were generated as previously described (Yokota et al., 1999). *Kit*$^{W\text{-}sh/W\text{-}sh}$ mice were obtained from Dr. H. Suto (Juntendo University). MaS-TRECK and BaS-TRECK mice were established as previously reported (Sawaguchi et al., 2012). All mice were maintained under SPF or GF conditions at the Experimental Animal Facility of the Institute of Medical Science, the University of Tokyo. All experiments were approved by the Animal Care and Use Committee of the University of Tokyo.

In Vivo Treatment

To remove DCs, we intraperitoneally treated *Itgax*-DTR mice with DT (500 ng, Sigma-Aldrich) (Jung et al., 2002). To deplete MCs and basophils, we injected MaS-TRECK and BaS-TRECK mice intraperitoneally with 250 ng DT for 5 consecutive days and then with 150 ng DT every other day (Sawaguchi et al., 2012). Mice were orally inoculated with 0.4% RA (Sigma-Aldrich) in corn oil (Wako) twice a week. Liarozole (1 mg, intraperitoneally) or apyrase (1 U/ear, grade VII, Sigma-Aldrich, intradermally) was injected before RA treatment. Mice received a mixture of ampicillin (1 g/L; Sigma-Aldrich), vancomycin (500 mg/L; Shionogi), neomycin (1 g/L; Sigma-Aldrich), and metronidazole (1 g/ L; Sigma-Aldrich) in drinking water since 2 weeks before RA treatment (Obata et al., 2010). MCs were reconstituted in *Kit*$^{W\text{-}sh/W\text{-}sh}$ mice by intraperitoneal and intravenous (5×10^6 cells each) or intradermal (1×10^6 cells) injection of BMMCs.

Cell Preparations

Mononuclear cells from the small intestine, colon, PEC, lung, and skin were isolated, and BMMCs were obtained as previously described (Kurashima et al., 2012; Kurashima et al., 2007). To prepare stromal cells and fibroblasts, tissues were digested with EDTA and collagenase (Sigma-Aldrich) and adherent cells were passaged every 4 days (process repeated once). Before coculture with BMMCs, cells were treated with 10 ng/ml mitomycin C (Sigma-Aldrich) for 3 hr and washed twice with PBS. In some experiments, BMMCs were cytospinned (600 rpm, 4 min) and stained for 1 hr with alcian blue (Muto Pure Chemicals, Tokyo, Japan) and for 20 min with safranin (Muto Pure Chemicals). Inflammatory monocytes or macrophages were collected from PEC 3 days after intraperitoneal injection of 2 ml of 4% thioglycolate.

In Vitro Treatment

For MCP1 and TNF-α measurement, 2×10^5 cells were stimulated with 0.5 mM of ATP for 2 days. For IL-1β measurement, 2×10^5 cells were stimulated with 0.1 μg/mL LPS for 8 hr, followed by 0, 0.5, or 5 mM of ATP for 1 hr. Chemokine and cytokine production in the culture supernatant was measured with CBA inflammatory cytokine kit (BD Biosciences) and IL-1β ELISA (R&D Systems). To stimulate TLR2-mediated pathway, we cultured thioglycolate-induced monocytes and macrophages with Pam2CSK4 (0.2 μg/mL, InvivoGen). To measure ATP secretion from skin organ, we floated skin (8.0 mm square) with the epidermis side upward on 12-well plates containing 1 ml PBS and incubated on ice for 10 min. ATP concentration in the culture was measured by ATP luciferase assay (PerkinElmer) (Kawamura et al., 2012; Kurashima et al., 2012).

Flow Cytometry

Cells were incubated with 5 μg/ml of anti-CD16/32 antibody (Biolegend) for 5 min and then stained for 30 min at 4°C with fluorescence-labeled antibodies; c-kit (0.2 μg/mL), Gr-1 (0.4 μg/mL), CD4 (1 μg/mL), CD11b (0.2 μg/mL), CD11c (0.4 μg/mL), and B220 (0.4 μg/mL) (BD Biosciences); FcεRIα (0.4 μg/mL) and CD207 (0.4 μg/mL) (eBioscience); and F4/80 (20 μg/mL) and ER-TR7 (5 μg/mL) (Abcam), and P2X7 (2 μg/mL, clone 1F11) (Kurashima et al., 2012). Flow cytometric analysis and cell sorting were performed with FACSCalibur and FACSAria (BD Biosciences), respectively.

Histology and Scoring

Skin samples were fixed in 4% paraformaldehyde and embedded in paraffin. Tissue sections (5 μm) were stained with hematoxylin and eosin (Wako). To

stain collagen$^+$ fibroblasts, we stained tissue sections with anilin blue orange G solution (Muto Pure Chemicals) for 1 hr and counterstained with toluidine blue (Wako) for 20 min. For the staining with anti-mouse cathelicidin antibody (Abcam), tissue sections were retrieved with Retrievagen A (BD Biosciences).

Inflammation severity was scored as follows: 0, no; 1, minimal; 2, mild; 3, moderate; and 4, marked. The slides were blinded, randomized, and reread to determine score. The total score was calculated as the sum of scores for inflammation, neutrophil number, mononuclear cell number, edema, and epithelial hyperplasia (Otsuka et al., 2011).

Whole-Mount FISH

Skin was fixed in 4% paraformaldehyde at 4°C overnight and washed with PBS for 7 hr. Tissues were hybridized with 10 μg/mL of Alexa 488-conjugated DNA probe (EUB338, Invitrogen) in a hybridization buffer (0.9 M NaCl, 20 mM Tris-HCl, 0.1% SDS, and 10 μg/mL) at 42°C overnight. After washing twice in a washing buffer (0.45 M NaCl, 20 mM Tris-HCl, 0.01% SDS) at 42°C for 10 min, tissues were flushed with PBS and observed by confocal microscopy (DM IRE2/TCS SP2, Leica) (Obata et al., 2010).

Microarray Analysis

Total RNA was prepared with RNeasy kit (QIAGEN). cRNA was hybridized with DNA probes on a GeneChip Mouse Genome 430 2.0 array (Affymetrix) (Kunisawa et al., 2013). Data were analyzed with GeneSpring 7.3.1 software (Silicon Genetics).

Quantitative RT-PCR

Total RNA was prepared with TRIzol (Invitrogen) and reverse transcribed by Superscript VILO (Invitrogen). Quantitative RT-PCR was performed with the LightCycler 480 II (Roche) and the Universal Probe Library (Roche). Primer sequence is available in Table S1.

Statistical Analysis

Statistical analysis was performed with the unpaired two-tailed Student's t test and Welch's t test. In some experiments, one-way ANOVA and Tukey's method were employed as indicated in figure legends.

SUPPLEMENTAL INFORMATION

Supplemental Information includes one table and five figures and can be found with this article online at http://dx.doi.org/10.1016/j.immuni.2014.01.014.

AUTHOR CONTRIBUTIONS

Y. Kurashima conducted the research, performed experiments, and wrote the manuscript. T.A., K.F., Y. Kogure, Y.S., and E.H. performed gene expression and animal experiments. N.S. conducted in situ experiments. K.K. and A.O. contributed to the experimental design, skin analysis, and histological scoring. M.K., S.A., and S.S. helped construct the transgenic mice. T.S. conducted the morphological analysis of MCs. K.M., J.K., and H.K. supervised the project and wrote the manuscript.

ACKNOWLEDGMENTS

We thank H. Suto (Atopy Research Center, Juntendo University, Tokyo) for providing *Kit*$^{W\text{-}sh/W\text{-}sh}$ mice, and S. Nakae (University of Tokyo) for advice on analyzing *Kit*$^{W\text{-}sh/W\text{-}sh}$ mice. We also thank Y. Yokota (School of Medicine, University of Fukui, Fukui) for providing *Id2*$^{-/-}$ mice. This work was supported by grants from the Ministry of Education, Science, Sports, and Technology of Japan (Grant-in Aid for Scientific Research S [H.K.] for Scientific Research on Innovative Areas [J.K.]; grant from the Leading-edge Research Infrastructure Program [to J.K., H.K.]); from the Young Researcher Overseas Visits Program for Vitalizing Brain Circulation (Japan Society for the Promotion of Science, J.K., H.K., Y.K.); for Japan Society for the Promotion of Science Fellows (Y.K., T.A., N.S.); from the Ministry of Health and Welfare of Japan (J.K., H.K.); from the Global Center of Excellence Program of the Center of Education and Research for Advanced Genome-based Medicine (H.K.); from the Program for Promotion of Basic and Applied Research for Innovations in Bio-oriented Industry (to J.K.); and Kowa Life Science Foundation (J.K.); Kishimoto Foundation Research Grant (J.K.); and from the Yakult Bioscience Foundation (J.K.).

Received: June 25, 2013
Accepted: January 15, 2014
Published: April 10, 2014

REFERENCES

Biggs, L., Yu, C., Fedoric, B., Lopez, A.F., Galli, S.J., and Grimbaldeston, M.A. (2010). Evidence that vitamin D(3) promotes mast cell-dependent reduction of chronic UVB-induced skin pathology in mice. J. Exp. Med. *207*, 455–463.

Cetin, E.D., Savk, E., Uslu, M., Eskin, M., and Karul, A. (2009). Investigation of the inflammatory mechanisms in alopecia areata. Am. J. Dermatopathol. *31*, 53–60.

De Coster, R., Wouters, W., and Bruynseels, J. (1996). P450-dependent enzymes as targets for prostate cancer therapy. J. Steroid Biochem. Mol. Biol. *56* (1-6 Spec No), 133–143.

Di Meglio, P., Perera, G.K., and Nestle, F.O. (2011). The multitasking organ: recent insights into skin immune function. Immunity *35*, 857–869.

Di Virgilio, F. (2007). Liaisons dangereuses: P2X$_{(7)}$ and the inflammasome. Trends Pharmacol. Sci. *28*, 465–472.

Duncan, F.J., Silva, K.A., Johnson, C.J., King, B.L., Szatkiewicz, J.P., Kamdar, S.P., Ong, D.E., Napoli, J.L., Wang, J., King, L.E., Jr., et al. (2013). Endogenous retinoids in the pathogenesis of alopecia areata. J. Invest. Dermatol. *133*, 334–343.

Elssner, A., Duncan, M., Gavrilin, M., and Wewers, M.D. (2004). A novel P2X7 receptor activator, the human cathelicidin-derived peptide LL37, induces IL-1 beta processing and release. J. Immunol. *172*, 4987–4994.

Erridge, C. (2010). Endogenous ligands of TLR2 and TLR4: agonists or assistants? J. Leukoc. Biol. *87*, 989–999.

Feyerabend, T.B., Weiser, A., Tietz, A., Stassen, M., Harris, N., Kopf, M., Radermacher, P., Möller, P., Benoist, C., Mathis, D., et al. (2011). Cre-mediated cell ablation contests mast cell contribution in models of antibody- and T cell-mediated autoimmunity. Immunity *35*, 832–844.

Fisher, G.J., and Voorhees, J.J. (1996). Molecular mechanisms of retinoid actions in skin. FASEB J. *10*, 1002–1013.

García-Serrano, L., Gomez-Ferrería, M.A., Contreras-Jurado, C., Segrelles, C., Paramio, J.M., and Aranda, A. (2011). The thyroid hormone receptors modulate the skin response to retinoids. PLoS ONE *6*, e23825.

Geria, A.N., and Scheinfeld, N.S. (2008). Talarozole, a selective inhibitor of P450-mediated all-trans retinoic acid for the treatment of psoriasis and acne. Curr. Opin. Investig. Drugs *9*, 1228–1237.

Gilfillan, A.M., and Beaven, M.A. (2011). Regulation of mast cell responses in health and disease. Crit. Rev. Immunol. *31*, 475–529.

Gurish, M.F., and Austen, K.F. (2012). Developmental origin and functional specialization of mast cell subsets. Immunity *37*, 25–33.

Hacker, C., Kirsch, R.D., Ju, X.S., Hieronymus, T., Gust, T.C., Kuhl, C., Jorgas, T., Kurz, S.M., Rose-John, S., Yokota, Y., and Zenke, M. (2003). Transcriptional profiling identifies Id2 function in dendritic cell development. Nat. Immunol. *4*, 380–386.

Hall, J.A., Grainger, J.R., Spencer, S.P., and Belkaid, Y. (2011). The role of retinoic acid in tolerance and immunity. Immunity *35*, 13–22.

Heiss, K., Jänner, N., Mähnss, B., Schumacher, V., Koch-Nolte, F., Haag, F., and Mittrücker, H.W. (2008). High sensitivity of intestinal CD8$^+$ T cells to nucleotides indicates P2X7 as a regulator for intestinal T cell responses. J. Immunol. *181*, 3861–3869.

Idzko, M., Hammad, H., van Nimwegen, M., Kool, M., Willart, M.A., Muskens, F., Hoogsteden, H.C., Luttmann, W., Ferrari, D., Di Virgilio, F., et al. (2007). Extracellular ATP triggers and maintains asthmatic airway inflammation by activating dendritic cells. Nat. Med. *13*, 913–919.

Izawa, K., Yamanishi, Y., Maehara, A., Takahashi, M., Isobe, M., Ito, S., Kaitani, A., Matsukawa, T., Matsuoka, T., Nakahara, F., et al. (2012). The receptor LMIR3 negatively regulates mast cell activation and allergic responses by binding to extracellular ceramide. Immunity *37*, 827–839.

Jin, H., Kumar, L., Mathias, C., Zurakowski, D., Oettgen, H., Gorelik, L., and Geha, R. (2009). Toll-like receptor 2 is important for the T(H)1 response to cutaneous sensitization. J Allergy Clin Immunol *123*, 875–882, e871.

Jung, S., Unutmaz, D., Wong, P., Sano, G., De los Santos, K., Sparwasser, T., Wu, S., Vuthoori, S., Ko, K., Zavala, F., et al. (2002). In vivo depletion of CD11c+ dendritic cells abrogates priming of $CD8^+$ T cells by exogenous cell-associated antigens. Immunity *17*, 211–220.

Junger, W.G. (2011). Immune cell regulation by autocrine purinergic signalling. Nat. Rev. Immunol. *11*, 201–212.

Kawamura, T., Ogawa, Y., Nakamura, Y., Nakamizo, S., Ohta, Y., Nakano, H., Kabashima, K., Katayama, I., Koizumi, S., Kodama, T., et al. (2012). Severe dermatitis with loss of epidermal Langerhans cells in human and mouse zinc deficiency. J. Clin. Invest. *122*, 722–732.

Kull, I., Bergström, A., Melén, E., Lilja, G., van Hage, M., Pershagen, G., and Wickman, M. (2006). Early-life supplementation of vitamins A and D, in water-soluble form or in peanut oil, and allergic diseases during childhood. J. Allergy Clin. Immunol. *118*, 1299–1304.

Kunisawa, J., Gohda, M., Hashimoto, E., Ishikawa, I., Higuchi, M., Suzuki, Y., Goto, Y., Panea, C., Ivanov, , II, Sumiya, R., et al. (2013). Microbe-dependent $CD11b^+$ IgA plasma cells mediate robust early-phase intestinal IgA responses in mice. Nat Commun *4*, 1772.

Kurashima, Y., Kunisawa, J., Higuchi, M., Gohda, M., Ishikawa, I., Takayama, N., Shimizu, M., and Kiyono, H. (2007). Sphingosine 1-phosphate-mediated trafficking of pathogenic Th2 and mast cells for the control of food allergy. J. Immunol. *179*, 1577–1585.

Kurashima, Y., Amiya, T., Nochi, T., Fujisawa, K., Haraguchi, T., Iba, H., Tsutsui, H., Sato, S., Nakajima, S., Iijima, H., et al. (2012). Extracellular ATP mediates mast cell-dependent intestinal inflammation through P2X7 purinoceptors. Nat Commun *3*, 1034.

Lunderius-Andersson, C., Enoksson, M., and Nilsson, G. (2012). Mast Cells Respond to Cell Injury through the Recognition of IL-33. Front Immunol *3*, 82.

Masuda, A., Nakamura, A., Maeda, T., Sakamoto, Y., and Takai, T. (2007). Cis binding between inhibitory receptors and MHC class I can regulate mast cell activation. J. Exp. Med. *204*, 907–920.

Matsushima, H., Yamada, N., Matsue, H., and Shimada, S. (2004). TLR3-, TLR7-, and TLR9-mediated production of proinflammatory cytokines and chemokines from murine connective tissue type skin-derived mast cells but not from bone marrow-derived mast cells. J. Immunol. *173*, 531–541.

Mizumoto, N., Kumamoto, T., Robson, S.C., Sévigny, J., Matsue, H., Enjyoji, K., and Takashima, A. (2002). CD39 is the dominant Langerhans cell-associated ecto-NTPDase: modulatory roles in inflammation and immune responsiveness. Nat. Med. *8*, 358–365.

Morizane, S., Yamasaki, K., Kabigting, F.D., and Gallo, R.L. (2010). Kallikrein expression and cathelicidin processing are independently controlled in keratinocytes by calcium, vitamin D(3), and retinoic acid. J. Invest. Dermatol. *130*, 1297–1306.

Naik, S., Bouladoux, N., Wilhelm, C., Molloy, M.J., Salcedo, R., Kastenmuller, W., Deming, C., Quinones, M., Koo, L., Conlan, S., et al. (2012). Compartmentalized control of skin immunity by resident commensals. Science *337*, 1115–1119.

Nakamura, Y., Franchi, L., Kambe, N., Meng, G., Strober, W., and Núñez, G. (2012). Critical role for mast cells in interleukin-1β-driven skin inflammation associated with an activating mutation in the nlrp3 protein. Immunity *37*, 85–95.

Obata, T., Goto, Y., Kunisawa, J., Sato, S., Sakamoto, M., Setoyama, H., Matsuki, T., Nonaka, K., Shibata, N., Gohda, M., et al. (2010). Indigenous opportunistic bacteria inhabit mammalian gut-associated lymphoid tissues and share a mucosal antibody-mediated symbiosis. Proc. Natl. Acad. Sci. USA *107*, 7419–7424.

Okano, J., Lichti, U., Mamiya, S., Aronova, M., Zhang, G., Yuspa, S.H., Hamada, H., Sakai, Y., and Morasso, M.I. (2012). Increased retinoic acid levels through ablation of Cyp26b1 determine the processes of embryonic skin barrier formation and peridermal development. J. Cell Sci. *125*, 1827–1836.

Otsuka, A., Kubo, M., Honda, T., Egawa, G., Nakajima, S., Tanizaki, H., Kim, B., Matsuoka, S., Watanabe, T., Nakae, S., et al. (2011). Requirement of interaction between mast cells and skin dendritic cells to establish contact hypersensitivity. PLoS ONE *6*, e25538.

Sandig, H., and Bulfone-Paus, S. (2012). TLR signaling in mast cells: common and unique features. Front Immunol *3*, 185.

Sawaguchi, M., Tanaka, S., Nakatani, Y., Harada, Y., Mukai, K., Matsunaga, Y., Ishiwata, K., Oboki, K., Kambayashi, T., Watanabe, N., et al. (2012). Role of mast cells and basophils in IgE responses and in allergic airway hyperresponsiveness. J. Immunol. *188*, 1809–1818.

Schirmer, C., Klein, C., von Bergen, M., Simon, J.C., and Saalbach, A. (2010). Human fibroblasts support the expansion of IL-17-producing T cells via up-regulation of IL-23 production by dendritic cells. Blood *116*, 1715–1725.

Sudo, N., Tanaka, K., Koga, Y., Okumura, Y., Kubo, C., and Nomoto, K. (1996). Extracellular ATP activates mast cells via a mechanism that is different from the activation induced by the cross-linking of Fc receptors. J. Immunol. *156*, 3970–3979.

Takahashi, T., Kimura, Y., Niwa, K., Ohmiya, Y., Fujimura, T., Yamasaki, K., and Aiba, S. (2013). In vivo imaging demonstrates ATP release from murine keratinocytes and its involvement in cutaneous inflammation after tape stripping. J. Invest. Dermatol. *133*, 2407–2415.

Takano, H., Nakazawa, S., Okuno, Y., Shirata, N., Tsuchiya, S., Kainoh, T., Takamatsu, S., Furuta, K., Taketomi, Y., Naito, Y., et al. (2008). Establishment of the culture model system that reflects the process of terminal differentiation of connective tissue-type mast cells. FEBS Lett. *582*, 1444–1450.

Tsai, M., Grimbaldeston, M., and Galli, S.J. (2011). Mast cells and immunoregulation/immunomodulation. Adv. Exp. Med. Biol. *716*, 186–211.

Varani, J., Fligiel, H., Zhang, J., Aslam, M.N., Lu, Y., Dehne, L.A., and Keller, E.T. (2003). Separation of retinoid-induced epidermal and dermal thickening from skin irritation. Arch. Dermatol. Res. *295*, 255–262.

Wang, Z., MacLeod, D.T., and Di Nardo, A. (2012). Commensal bacteria lipoteichoic acid increases skin mast cell antimicrobial activity against vaccinia viruses. J. Immunol. *189*, 1551–1558.

Wilhelm, K., Ganesan, J., Müller, T., Dürr, C., Grimm, M., Beilhack, A., Krempl, C.D., Sorichter, S., Gerlach, U.V., Jüttner, E., et al. (2010). Graft-versus-host disease is enhanced by extracellular ATP activating P2X7R. Nat. Med. *16*, 1434–1438.

Xing, W., Austen, K.F., Gurish, M.F., and Jones, T.G. (2011). Protease phenotype of constitutive connective tissue and of induced mucosal mast cells in mice is regulated by the tissue. Proc. Natl. Acad. Sci. USA *108*, 14210–14215.

Yamasaki, K., Di Nardo, A., Bardan, A., Murakami, M., Ohtake, T., Coda, A., Dorschner, R.A., Bonnart, C., Descargues, P., Hovnanian, A., et al. (2007). Increased serine protease activity and cathelicidin promotes skin inflammation in rosacea. Nat. Med. *13*, 975–980.

Yokota, Y., Mansouri, A., Mori, S., Sugawara, S., Adachi, S., Nishikawa, S., and Gruss, P. (1999). Development of peripheral lymphoid organs and natural killer cells depends on the helix-loop-helix inhibitor Id2. Nature *397*, 702–706.

Published OnlineFirst September 3, 2014; DOI: 10.1158/0008-5472.CAN-14-0471

Molecular and Cellular Pathobiology

Cancer Research

Stress Response Protein Cirp Links Inflammation and Tumorigenesis in Colitis-Associated Cancer

Toshiharu Sakurai[1], Hiroshi Kashida[1], Tomohiro Watanabe[2], Satoru Hagiwara[1], Tsunekazu Mizushima[3], Hideki Iijima[4], Naoshi Nishida[1], Hiroaki Higashitsuji[5], Jun Fujita[5], and Masatoshi Kudo[1]

Abstract

Colitis-associated cancer (CAC) is caused by chronic intestinal inflammation and is reported to be associated with refractory inflammatory bowel disease (IBD). Defective apoptosis of inflammatory cell populations seems to be a relevant pathogenetic mechanism in refractory IBD. We assessed the involvement of stress response protein cold-inducible RNA-binding protein (Cirp) in the development of intestinal inflammation and CAC. In the colonic mucosa of patients with ulcerative colitis, expression of Cirp correlated significantly with the expression of TNFα, IL23/IL17, antiapoptotic proteins Bcl-2 and Bcl-xL, and stem cell markers such as Sox2, Bmi1, and Lgr5. The expression of Cirp and Sox2 was enhanced in the colonic mucosae of refractory ulcerative colitis, suggesting that Cirp expression might be related to increased cancer risk. In human CAC specimens, inflammatory cells expressed Cirp protein. *Cirp*$^{-/-}$ mice given dextran sodium sulfate exhibited decreased susceptibility to colonic inflammation through decreased expression of TNFα, IL23, Bcl-2, and Bcl-xL in colonic lamina propria cells compared with similarly treated wild-type (WT) mice. In the murine CAC model, Cirp deficiency decreased the expression of TNFα, IL23/IL17, Bcl-2, Bcl-xL, and Sox2 and the number of Dclk1^{+} cells, leading to attenuated tumorigenic potential. Transplantation of *Cirp*$^{-/-}$ bone marrow into WT mice reduced tumorigenesis, indicating the importance of Cirp in hematopoietic cells. Cirp promotes the development of intestinal inflammation and colorectal tumors through regulating apoptosis and production of TNFα and IL23 in inflammatory cells. *Cancer Res; 74(21); 6119–28. ©2014 AACR.*

Introduction

The inflammatory bowel diseases (IBD)—ulcerative colitis and Crohn disease—are thought to result from aberrant activation of the intestinal mucosal immune system (1). Although the pathogenesis of IBD remains unclear, a number of studies have suggested the involvement of abnormal apoptosis in intestinal epithelial cells, resulting from increased production of cytokines, such as TNF, ILs, and IFNs (2). TNFα is a key mediator of inflammation in IBD and has been the primary target of biologic therapies (3). This cytokine induces inflammation by promoting the production of IL1β and IL6, expression of adhesion molecules, proliferation of fibroblasts, activation of procoagulant factors, and cytotoxicity of the acute phase response (4). The IL23/T_H17 (T-helper IL17–producing cell) pathway has been identified to play a critical role in IBD. IL23 has been shown to promote the expansion of a distinct lineage of T_H17 cells that are characterized by production of a number of specific cytokines not produced by T_H1 or T_H2 cells, including IL17A, IL17F, IL21, and IL22 (5). IL23/IL17 signaling enhances the immunosuppressive activity of regulatory T cells and reduces CD8^{+} cells in tumor, leading to enhanced tumor initiation and promotion (6, 7). Recently, a study has suggested that colorectal cancer tissue–derived Foxp3^{+} IL17^{+} cells have the capacity to induce cancer-initiating cells *in vitro* (8). The most conspicuous link between inflammation and colon cancer is seen in patients with IBD (9), and development of colorectal cancer is one of the most serious complications of IBD, which is also referred to as colitis-associated cancer (CAC; ref. 10). Thus, it is of great importance to improve our understanding of the molecular link between chronic inflammation and CAC to identify a target molecule with therapeutic potential for the treatment of IBD and prevention of CAC.

It is widely accepted that most tumors harbor cancer stem cells, which are crucial for a tumor's evolutionary capability. Cancer stem cells resemble normal stem cells in their capacity to self-renew and continuously replenish tumor progeny (11, 12). The G-protein–coupled receptor Lgr5 and the polycomb group protein Bmi1 are 2 recently described molecular markers of the self-renewing multipotent adult stem cell populations residing in intestinal crypts that mediate regeneration of the intestinal epithelium (13, 14). Pluripotency-

[1]Department of Gastroenterology and Hepatology, Kinki University Faculty of Medicine, Osaka-Sayama, Japan. [2]Center for Innovation in Immunoregulative Technology and Therapeutics, Graduate School of Medicine, Kyoto University, Kyoto, Japan. [3]Department of Surgery, Osaka University, Osaka, Japan. [4]Department of Gastroenterology and Hepatology, Osaka University, Osaka, Japan. [5]Department of Clinical Molecular Biology, Graduate School of Medicine, Kyoto University, Kyoto, Japan.

Note: Supplementary data for this article are available at Cancer Research Online (http://cancerres.aacrjournals.org/).

Corresponding Author: Toshiharu Sakurai, Department of Gastroenterology and Hepatology, Kinki University Faculty of Medicine, 377-2 Ohno-Higashi, Osaka-Sayama, Osaka 589-8511, Japan. Phone: 81-72-3660221, ext. 3525; Fax: 81-72-3672880; E-mail: sakurai@med.kindai.ac.jp

doi: 10.1158/0008-5472.CAN-14-0471

©2014 American Association for Cancer Research.

Downloaded from cancerres.aacrjournals.org on April 16, 2015. © 2014 American Association for Cancer Research.

Published OnlineFirst September 3, 2014; DOI: 10.1158/0008-5472.CAN-14-0471

associated transcription factors like Sox2 are known to regulate cellular identity in embryonic stem cells. Sox2 expression specifically increased the numbers of stem cells and repressed Cdx2, a master regulator of endodermal identity. *In vivo* studies demonstrated that Sox21, another member of the SoxB gene family, was a specific, immediate, and cell-autonomous target of Sox2 in intestinal stem cells (15). Sox2 participates in the reprogramming of adult somatic cells to a pluripotent stem cell state and is implicated in tumorigenesis in various organs (16).

Cold-inducible RNA-binding protein (Cirp, also called Cirbp or hnRNP A18) was originally identified in the testis as the first mammalian cold shock protein (17) and is suggested to mediate the preservation of neural stem cells (18). Cirp is induced by cellular stresses such as UV irradiation and hypoxia (19–21). In response to the stress, Cirp, which migrates from the nucleus to the cytoplasm, affects posttranscription expression of its target mRNAs (22–24) and functions as a damage-associated molecular pattern molecule that promotes inflammatory responses when present extracellularly (25). Cirp also affects cell growth and cell death induced by TNFα or genotoxic stress (26, 27). However, the involvement of Cirp in colitis and CAC is not well understood.

Here, we examined whether Cirp plays a role in inflammatory immune responses and tumorigenesis in the gut by using a murine CAC model of Cirp-deficient ($Cirp^{-/-}$) mice and found that Cirp promoted colitis and colorectal tumorigenesis by inhibiting apoptosis and increasing TNFα and IL23 production in inflammatory cells. In patients with ulcerative colitis, refractory inflammation is associated with increased Cirp expression in the colonic mucosa, which would increase the risk for CAC. This study represents the first report of the functional link between Cirp and intestinal tumorigenesis.

Materials and Methods

Human tissue samples

In total, 236 colonic mucosa specimens were obtained by endoscopy or surgery from patients with ulcerative colitis, including 67 cases of refractory ulcerative colitis, 98 cases of nonrefractory active ulcerative colitis, and 20 cases in remission, as well as 21 colonic mucosa of patients with Crohn disease and 30 normal colonic mucosa specimens from controls without IBD. Refractory ulcerative colitis was defined according to endoscopic criteria and categorized as being active for more than 6 months. Active inflammation was defined as Mayo endoscopic score ≥2. CAC specimens were obtained from 10 patients who had undergone colorectal resection. The clinical study protocol conformed to the ethical guidelines of the 1975 Declaration of Helsinki and was approved by the relevant institutional review boards.

Mice and treatment

$Cirp^{-/-}$ mice showing neither gross abnormality nor colonic inflammation were used as a murine CAC model. The generation of $Cirp^{-/-}$ mice has been described previously (28). Sex- and age-matched C57BL/6 wild-type (WT) and $Cirp^{-/-}$ mice (8–12 weeks old) received 2.5% (w/v) dextran sodium sulfate (DSS; molecular weight, 36,000–50,000 kDa; MP Biomedicals) in drinking water. Mice were intrapertioneally injected with 20 mg/kg anti- TNFα antibody (#16-7423, eBioscience) or an IgG isotype control before DSS treatment.

Isolation of lamina propria cells was performed as described previously (29). The isolated cells were sorted using immunomagnetic beads coated with monoclonal antibodies against CD11b (MACS Beads, Miltenyi Biotec) with the help of a separation column and a magnetic separator from the same company in accordance with the manufacturer's recommendations for isolating murine macrophages.

As the protocol for the murine CAC model, mice were intraperitoneally injected with 12.5 mg/kg azoxymethane (AOM; Sigma-Aldrich). After 5 days, 2.0% DSS was included in the drinking water for 5 days, followed by 16 days of regular water. This cycle was repeated 3 times. Then, 1.5% DSS was included in the drinking water for 4 days, followed by 7 days of regular water. Upon sacrifice, the colon was excised from the ileocecal junction to the anus, cut open longitudinally, and prepared for histologic evaluation. Colons were assessed macroscopically for polyps under a dissecting microscope.

Bone marrow transplantation (BMT) experiments were performed as previously described, with slight modifications (30). Bone marrow from the tibia and femur was washed twice in Hank balanced salt solution, and 10^7 bone marrow cells were injected into the tail vein of lethally irradiated (11 Gy) recipient mice. Eight weeks posttransplantation, the mice were subjected to the murine CAC protocol. Bone marrow cells were grown in culture dishes in the presence of macrophage colony-stimulating factor (M-CSF; 10 ng/mL) and then differentiated to bone marrow–derived macrophages in 10 days. All animal procedures were performed according to approved protocols and in accordance with the recommendations for the proper care and use of laboratory animals. The animal study protocol was approved by the Medical Ethics Committee of Kinki University School of Medicine (Osaka-Sayama, Japan).

Colonic injury scoring

Excised colons were rolled up and fixed in 10% formaldehyde, embedded in paraffin, and stained with hematoxylin and eosin (H&E). The degree of colonic injury was assessed by histologic scoring as described previously (31), with minor modifications. The protocol is described in detail in Supplementary Materials and Methods.

Biochemical and immunochemical analyses

Real-time qPCR, immunoblotting, and immunohistochemistry were previously described (32). Primer sequences are given in Supplementary Materials and Methods. The following antibodies were used: anti-actin and anti-DCAMLK1 (Dclk1) from Sigma-Aldrich; anti-Bcl-2, anti-phospho-IκBα, anti-IκBα, anti-phospho-ERK, anti-ERK, anti-Sox2, anti-E-cadherin, anti-PCNA from Cell Signaling; and anti-F4/80 from eBioscience. Generation of anti-Cirp polyclonal antibody was previously described (28). Immunohistochemistry was performed using ImmPRESS reagents (Vector Laboratory) according to the manufacturer's recommendations. Immunofluorescent terminal deoxynucleotidyl transferase–mediated dUTP nick end labeling (TUNEL) staining was performed to measure

Downloaded from cancerres.aacrjournals.org on April 16, 2015. © 2014 American Association for Cancer Research.

Published OnlineFirst September 3, 2014; DOI: 10.1158/0008-5472.CAN-14-0471

apoptosis in paraffin-embedded sections using the In Situ Apoptosis Detection Kit as described by the manufacturer (Takara). Nuclei were stained with 4,6′-diamidino-2-phenylindole to count the total cells per crypt. A minimum of 10 crypts were counted per section.

Statistical analysis

Differences were analyzed using the Student *t* test. To compare variables of more than 2 conditions, ANOVO with *post hoc* Tukey–Kramer honestly significant difference (HSD) multiple comparison was applied. The relationship between the expression of several genes was analyzed by Spearman rank correlation test. $P < 0.05$ was considered significant.

Results

Correlation of Cirp expression with TNFα, IL23/IL17, Bcl-2, and stem cell marker expression in patients with IBD

Cirp expression correlated weakly but significantly with TNFα with a linear coefficient of 0.26 in the colonic mucosa of patients with ulcerative colitis (Supplementary Fig. S1A). In patients with Crohn disease, Cirp expression did not significantly correlate with TNFα (data not shown) probably because the majority of patients with Crohn disease enrolled in this study had undergone anti-TNFα therapy. IL23p19 is the specific subunit of IL23, a positive regulator of T_H17 and other IL17-producing cells (5). A significant correlation was found between *Cirp* and *IL17A* or *IL23p19* mRNA expression in patients with ulcerative colitis (Supplementary Fig. S1B and S1C) and in patients with Crohn disease (Supplementary Fig. S2A).

Defective apoptosis of inflammatory cell populations regulated by Bcl-2 seems to be a relevant pathogenetic mechanism in IBD (33, 34). There was a significant correlation between Cirp and Bcl-2 expression with a linear coefficient of 0.76 in patients with ulcerative colitis and with a linear coefficient of 0.60 in patients with Crohn disease (Fig. 1A and Supplementary Fig. S2B). Expression of Bcl-xL, another antiapoptotic protein, was significantly correlated with that of Cirp with a linear coefficient of 0.60 in patients with ulcerative colitis (Supplementary Fig. S1D) and with a linear coefficient of 0.85 in patients with Crohn disease (Supplementary Fig. S2C).

Stem cells, characterized by their ability to self-renew indefinitely and produce progeny capable of repopulating tissue-specific lineages, are critical for maintaining normal tissue homeostasis (35). Cirp is suggested to mediate the preservation of neural stem cells (18). Cirp expression correlated with Sox2, Bmi1, Lgr5, and Dclk1 levels with linear coefficients of 0.62, 0.45, 0.42, and 0.25, respectively, in patients with ulcerative colitis (Fig. 1B–D and Supplementary Fig. S1E) and correlated with Sox2 with a linear coefficient of 0.63 in patients with Crohn disease (Supplementary Fig. S2D). Cirp might be involved in regulation of intestinal inflammation and homeostasis maintenance in patients with IBD.

Increased Cirp expression in the colonic mucosa of patients with refractory ulcerative colitis

We next explored whether an association exists between Cirp expression and the clinical status of patients with ulcerative colitis. Refractory and nonrefractory active ulcerative colitis could not be distinguished by endoscopic findings (Fig. 2A). Cirp expression levels were specifically increased in patients with refractory ulcerative colitis associated with long-term inflammation, whereas similar expression levels of Cirp were found between normal colonic mucosa and the mucosa of patients with nonrefractory active ulcerative colitis (Fig. 2B). Similarly, increased Sox2 expression levels were found in the colonic mucosa of patients with refractory IBD (Fig. 2C). Immunohistochemistry showed that Sox2 was expressed in the mesenchyme and Dclk1 was expressed in the crypt of patients with refractory ulcerative colitis (Supplementary Fig. S3A and S3D). In contrast, increased TNFα expression was found in the colonic mucosa of both refractory and nonrefractory active ulcerative colitis (Fig. 2D). Immunohistochemistry was performed to identify the cells expressing Cirp in the human intestine, and inflammatory cells were found to express more Cirp protein than epithelial cells, whose expression pattern was similar in controls and patients with ulcerative colitis. In chronically inflamed mucosa, Cirp expression was enhanced in inflammatory cells (Fig. 2E and Supplementary Fig. S3B). Inflammatory cells preferentially but not exclusively expressed Cirp protein also in human CAC cases (Supplementary Fig. S3C).

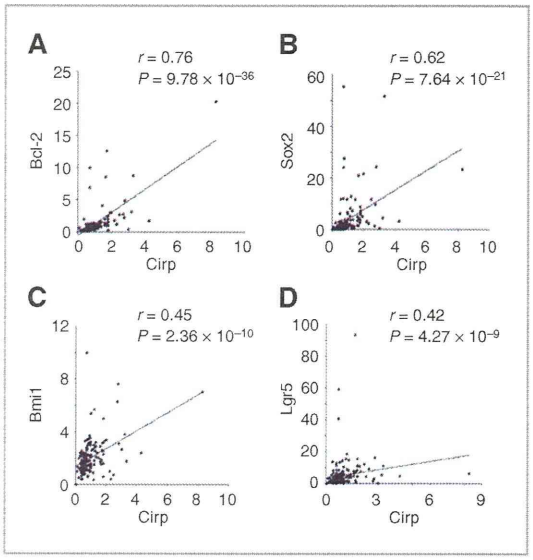

Figure 1. Association between Cirp and the expression of Bcl-2 and various stem cell markers in the colonic mucosa of patients with ulcerative colitis. Scatter plot of relative mRNA levels of Cirp and the respective genes (A, Bcl-2; B, Sox2; C, Bmi1; D, Lgr5) in human colonic mucosa.

Cirp$^{-/-}$ mice challenged with DSS have decreased susceptibility to inflammation

DSS-induced colitis is a murine model resembling human ulcerative colitis. Experimental colitis was induced by treating mice with 2.5% DSS. Histologic analysis revealed substantially less epithelial damage and disruption of crypt architecture in

Downloaded from cancerres.aacrjournals.org on April 16, 2015. © 2014 American Association for Cancer Research.

Published OnlineFirst September 3, 2014; DOI: 10.1158/0008-5472.CAN-14-0471

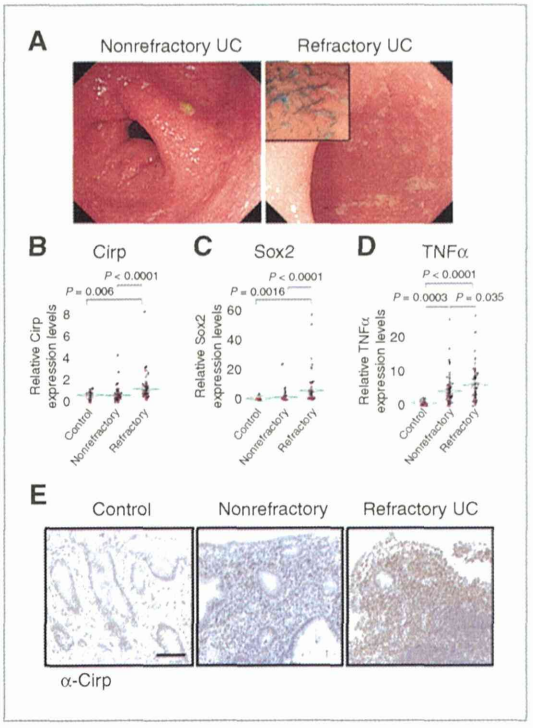

Figure 2. Cirp expression is increased in the colonic mucosa of patients with refractory ulcerative colitis (UC). A, endoscopic images of refractory and nonrefractory active ulcerative colitis specimens with a magnified inset. B–D, expression of *Cirp* (B), *Sox2* (C), and *TNFα* (D) mRNA in normal colonic mucosa (control, $n = 30$), colonic mucosa of patients with nonrefractory active ulcerative colitis (nonrefractory, $n = 98$), and those with refractory ulcerative colitis (refractory, $n = 67$), as determined by quantitative real-time qPCR. *P* values were calculated by *post hoc* Tukey–Kramer HSD multiple comparison. The *F* and *P* values for the ANOVO test are as follows: $F(2, 192) = 11.98$; $P < 0.0001$ (B), $F(2, 192) = 10.29$; $P < 0.0001$ (C), and $F(2, 192) = 13.70$; $P < 0.0001$ (D). E, representative images of immunohistochemical findings in human colonic mucosa of patients without ulcerative colitis and those with nonrefractory and refractory ulcerative colitis. Scale bar, 50 μm.

Cirp$^{-/-}$ mice than in WT mice (Fig. 3A), and inflammatory cell infiltration into the colon was less in *Cirp*$^{-/-}$ mice (Fig. 3B). Immunohistochemically assessed macrophage infiltration was smaller in *Cirp*$^{-/-}$ than in WT mice after DSS administration (Fig. 3C), and the epithelial injury score was significantly smaller in the *Cirp*$^{-/-}$ mice than in the controls (Fig. 3D). Next, we compared apoptosis induction in DSS-treated WT and *Cirp*$^{-/-}$ mice. Apoptosis detected by TUNEL staining was observed in DSS-treated mice, primarily in the colonic crypts (Fig. 3E), but was blocked by 50% in the *Cirp*$^{-/-}$ mice (Fig. 3F). Examination of the colonic lysates from DSS-treated WT and *Cirp*$^{-/-}$ mice showed that the Cirp presence increased PCNA expression in the colon (Supplementary Fig. S4A).

The associated immune response was investigated by analyzing colonic cytokine levels. Colonic tissue from *Cirp*$^{-/-}$ mice showed a smaller immune response with lower levels of proinflammatory cytokine TNFα and IL23 than that of WT mice (Fig. 4A–C), which is consistent with the data in humans (Fig. 1 and Supplementary Fig. S1). TNFα expression was upregulated in nonrefractory active ulcerative colitis whereas Cirp expression was not in these patients (Fig. 2B and D). This is probably because TNFα is induced in both a Cirp-dependent and -independent manners in the colon. There was no significant difference in IL1β, IL10, and IL21 (Fig. 4B and Supplementary Fig. S4B). To explore the mechanisms of the effects of Cirp on TNFα production, we sought to confirm these findings *in vitro*. In lamina propria cells isolated from DSS-treated colons of Cirp-deficient mice, expression of TNFα and IL23 was decreased compared with those of WT mice (Fig. 4D). TNFα is produced chiefly by activated macrophages, although it can be produced by many other cell types as lymphocytes and natural killer cells (36), so we next isolated macrophages from DSS-treated colons. TNFα mRNA expression was significantly reduced in Cirp-deficient macrophages (Fig. 4E). Macrophages

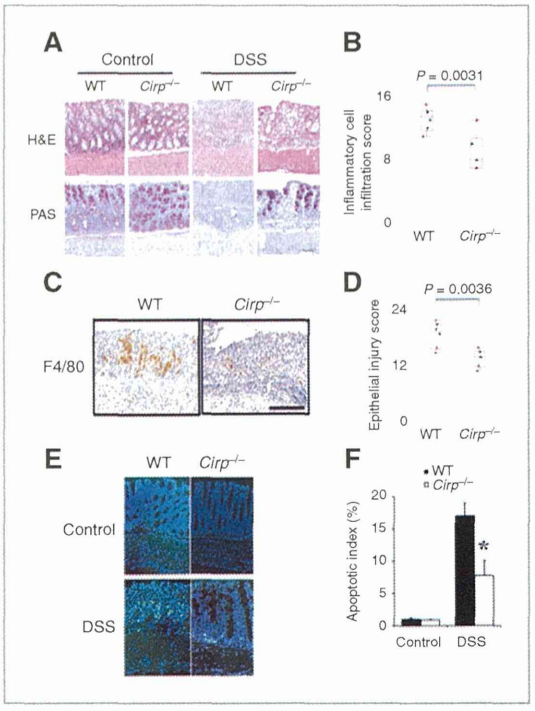

Figure 3. Susceptibility to inflammation is decreased in *Cirp*$^{-/-}$ mice challenged with DSS. A, representative photographs of H&E-stained and periodic acid—Schiff (PAS)-stained colons of WT and *Cirp*$^{-/-}$ mice 7 days after the initiation of DSS administration (original magnification, ×200). Scale bar, 50 μm. B, inflammatory cell infiltration into colonic tissues of WT and *Cirp*$^{-/-}$ mice 7 days after the initiation of DSS administration. Scoring was performed as described in Materials and Methods. $n = 6$ per group. C, representative images of immunohistochemical detection of F4/80, a marker for macrophages, in colonic tissue. Scale bar, 100 μm. D, histologic scoring of epithelial injury in colons. $n = 6$ per group. E, TUNEL staining of colonic tissues from DSS-treated mice (original magnification, ×200). F, the apoptotic index was measured by counting TUNEL signals in 100 randomly selected crypts. Results are expressed as means ± SEM ($n = 4$ per group). *, $P < 0.05$ compared with WT mice.

Downloaded from cancerres.aacrjournals.org on April 16, 2015. © 2014 American Association for Cancer Research.